Am J Transl Res 2023;15(4):2598-2609
www.ajtr.org /ISSN:1943-8141/AJTR0147125

Original Article

An immunogenic cell death-related classification predicts response to immunotherapy and prognosis in triple-negative breast cancer

Xu-Yu Cheng[1*], Yuan Liang[2,3,4,5*], Hong-Fei Zhang[1], Fang-Ze Qian[1], Xiao-Hu Sun[2,3], Xiao-An Liu[1]

[1]Department of Breast Surgery, The First Affiliated Hospital of Nanjing Medical University, Nanjing 210029, Jiangsu, China; [2]Hepatobiliary Center of The First Affiliated Hospital, Nanjing Medical University, Nanjing 210029, Jiangsu, China; [3]Research Unit of Liver Transplantation and Transplant Immunology, Chinese Academy of Medical Sciences, Nanjing 210029, Jiangsu, China; [4]School of Medicine, Southeast University, Nanjing 210029, Jiangsu, China; [5]School of Biological Science & Medical Engineering, Southeast University, Nanjing 210029, Jiangsu, China. [*]Equal contributors.

Received October 20, 2022; Accepted February 22, 2023; Epub April 15, 2023; Published April 30, 2023

Abstract: Objective: Immunogenic cell death (ICD) of tumor cells is characterized by the induction of adaptive and innate immune responses, which in turn activates the immune surveillance and improves the efficacy of immunotherapy. In this study, we aimed to investigate the effect of ICD on the prognosis and the efficacy of immunotherapy in patients with triple-negative breast cancer (TNBC). Methods: TNBC samples from The Cancer Genome Atlas-Breast Cancer (TCGA-BRCA) dataset were divided into two subtypes (ICD-high and ICD-low) based on the ICD status by using the consensus clustering method, and their genomic landscape and immune landscape were delineated. Furthermore, we established an ICD-related prognostic model to predict the efficacy of immunotherapy and the survival of TNBC. Results: Our study showed that a poor prognosis of TNBC was associated with ICD-high subtype, while a favorable outcome was associated with ICD-low subtype. The immune landscape profiling results revealed that ICD-high subtype presented an immune-hot phenotype, whereas ICD-low subtype was associated with an immune-cold phenotype. Furthermore, our prognostic model predicted that the high-risk score group had a poor overall survival (OS), which was consistent with the actual data in the Gene Expression Omnibus (GEO) dataset. We also used tumor immune dysfunction and exclusion (TIDE) to determine the predictive significance of our ICD risk signature in immunotherapy efficacy, and found that ICD high-risk group had the highest response rate to immunotherapy in the immunotherapy response group. Conclusion: Our results reveal a correlation between ICD status and alterations in the tumor immune microenvironment in patients with TNBC. This finding might help guide clinicians in immunotherapy application for TNBC patients.

Keywords: Immunogenic cell death, immunotherapy, TNBC, prognosis, tumor microenvironment

Introduction

Immunogenic cell death (ICD) is a type of cancer cell death that can trigger the host immune response and reshape the immunosuppressive tumor microenvironment (TME) by attracting innate and adaptive immune cells [1, 2]. ICD initiates adaptive immune responses by releasing damage-related molecular patterns (DAMPs) and the subsequent interaction of DAMPs with pattern recognition receptors (PRRs) expressed by innate immune cells [3, 4], which induces a cascade of cellular responses and triggers an adaptive immune response to kill tumor cells [3, 5-7]. In support of this notion, emerging preclinical evidence has shown that ICD can be used to reinforce the therapeutic effects [8-10]. However, the application of ICD in clinical practice remains to be fully determined, and further clinical studies should consider patients' clinical background to evaluate the efficacy of ICD [11, 12]. Therefore, identifying biomarkers that stratify patients who will benefit from ICD is important for precision immunotherapy.

Triple-negative breast cancer (TNBC) is the most malignant subtype of breast cancer (BC) with high recurrence rate and the worst prognosis [13]. The immune system is usually considered to be an important component of BC, with

TNBC being the most immunogenic subtype [14]. Since the TNBC lacks a specific therapeutic targets, chemotherapy has been the standard treatment for TNBC during the past decades, whereas immunotherapy, including immune checkpoint inhibitors (ICIs), antibody-drug conjugates, and adopted T-cell treatment is showing great potential in recent years [15, 16]. Likewise, recent studies have also shown that neoadjuvant therapy against breast cancer, including TNBC, might lead to antitumor immune memory acquisition and thus inhibit tumor recurrence [17, 18]. In addition to the development of cancer immunotherapy, investigating the effectiveness of the therapeutic strategy is another focus on the clinical application of immunotherapy. Accordingly, identifying biomarkers that can predict the efficacy of immunotherapy in TNBC is urgently needed.

In this study, we aimed to establish an ICD-associated prognostic model that predicts the prognosis of TNBC and to construct a new classification model for TNBC patients according to their ICD characteristics. Our findings may be helpful in guiding precision immunotherapy for TNBC.

Materials and methods

Data source and collection

The RNA-seq transcriptome and the corresponding clinical information of 116 TNBC patients and 114 normal samples were collected in the TCGA-BRCA database (https://cancergenome.nih.gov/) through the Xena platform (http://xena.ucsc.edu/) for the training cohort. Furthermore, we downloaded the expression profile, along with the clinical information of patients from GSE65194 (https://www.ncbi.nlm.nih.gov/geo/query/acc.cgi?acc=GSE65194) for the validation cohort.

Consensus clustering

The ConcensusClusterPlus (v1.60.0) R package was used to determine the reliable and stable clusters related to ICD. Subsequently, we assessed the number of rationalized clusters from k = 2 to 9 and replicated the above steps 1000 times to obtain realistic results. The above results were visualized by the heatmap (v1.0.12) R package.

Identification of differentially expressed genes

We used the Wilcoxon rank sum test algorithm to identify genes that were significantly differentially expressed between ICD-high and ICD-low groups. The differential expressed mRNAs was extracted when $P < 0.05$ and $|\log2 \text{(fold change)}| > 0.5$.

Pathway enrichment analysis

Gene Ontology (GO) and Kyoto Encyclopedia of Genes and Genomes (KEGG) analysis was conducted to identify the differentially enriched biological pathways between the ICD-low and ICD-high subtypes by using the cluster profile (v4.4.4) R package. Radar plots were used to display the results of GO and KEGG functional enrichment analysis.

Immune cell infiltration analysis between the ICD-high and ICD-low subtypes

To explore the immune cell composition in TNBC patients, we utilized TIMER v2.0 to estimate the fraction of 22 immune cell types in these samples, and the resulting TIMER values were defined as the immune cell infiltration composition of each sample. Furthermore, we compared the immune cell filtration of 22 immune cell types between the ICD-high and ICD-low groups.

Somatic mutation analysis

Somatic mutation data of the TNBC patients were acquired from TCGA Genomic Data Commons (GDC) Data Portal in “maf” format. We screened the top 30 frequently mutated genes in these samples, and waterfall plots were then conducted using the map tools (v2.12.0) R package.

Survival analysis

Kaplan-Meier (KM) analysis was performed to compare the overall survival (OS) between the ICD-high and ICD-low subtypes using the survminer (v 0.4.9) and survival (v3.2.7) R packages. The univariate Cox regression analysis was conducted to identify the prognostic values of the ICD-associated genes, while the multivariate Cox regression analysis was used to verify that the risk score as prognostic biomarker for OS in TNBC.

Development of the ICD-associated risk signature

The genes significantly associated with ICD that were identified by the univariate Cox regression analysis were then subjected to a (Least Absolute Shrinkage and Selection Operator) LASSO Cox regression analysis to construct an ICD-related risk signature. LASSO is a commonly used regression algorithm that can combine variable selection and regularization which improves the performance in the resulting statistical model.

Prediction of immunotherapy outcomes

Tumor immune dysfunction and exclusion (TIDE, http://tide.dfci.harvard.edu) analysis was employed to predict the different ICD-related risk scores between immunotherapeutic response and non-response groups.

Results

ICD-associated subtypes are related to clinical outcome

To determine the list of ICD-associated genes that will be used in our study, we extensively reviewed the literature and mostly referred to the study by Abhishek et al. Then, the expression of these ICD-associated genes was examined in TNBC and normal samples in the TCGA-BRCA cohort (**Figure 1A**). We found that most of the ICD-associated genes were abnormally expressed in TNBC samples, including FOXP3, CD4, IFNG, PRF1, CXCR3, CD8A, HMGB1, HSP90AA1, ATG5, IFNB1, BAX, PDIA3, CALR, MYD88, and TNF (**Figure 1B**). Furthermore, we used the consensus clustering analysis to identify clusters associated with ICD in these TNBC samples. Based on the distinct ICD gene expression pattern, we classified the TCGA cohort into two clusters after k-means clustering (**Figure 1C-E**). Specifically, the cluster C1 had high expression of ICD-related genes, representing a subtype of ICD-high, while the cluster C2 showed lower expression of ICD-related genes, representing a subtype of ICD-low (**Figure 1F**, **1G**). Moreover, overall survival analysis suggested that these two ICD-associated subtypes had different clinical outcomes, as a poor prognosis was associated with the ICD-high subtype, whereas a favorable outcome was associated with ICD-low subtype (**Figure 1G**).

Analysis of differentially expressed genes (DEGs) and key signaling pathways in each ICD subtype

Since these two ICD-associated subtypes exhibited differential prognosis, we sought to elucidate the mechanisms involved in the prognosis by examining the DEGs and the different key signaling pathways between these two subtypes. We identified 362 dysregulated genes in the ICD-high subtype (**Figure 2A**, **2B**), and the upregulated genes were enriched in pathways related to immune activity, including the cytokine-mediated signaling pathway, cellular response to interferon-gamma, chemokine-mediated signaling pathway, cytokine-cytokine receptor interaction, natural killer cell-mediated cytotoxicity, and chemokine signaling pathway (**Figure 2C**). This suggested that the ICD-high subtype was associated with an immune active microenvironment.

Differential genomic landscape between the ICD-low and ICD-high subtypes

We compared the genomic landscape between these two ICD subtypes and evaluated the tumor-intrinsic genomic changes in the ICD-high and ICD-low subtypes of the TCGA-TNBC cohort. The data indicated that the ICD-high subtype exhibited a significantly higher mutation rate of FLG, PDILT, and AHCTF1 than in the ICD-low subtype (**Figure 3A**, **3B**). In the TCGA-cohort, the ICD ssGSEA (gene set enrichment analysis) score was higher in the *CLIP2, KIF5C, SEMA4F, SGIP1,* and *SMAP1* mutant groups than in the wild-type groups, while the ICD ssGSEA score was lower in *AIRD1B, DUSO27, OR5I1,* and *OBSCN* mutated groups than in wild type groups ($P < 0.05$, **Figure 3C**). Furthermore, the ICD-low subtype had higher tumor mutation burden (TMB) levels compared to the ICD-high subtype (**Figure 3D**).

Notably, we assessed the co-occurrence and mutual exclusion mutations among the mutant genes with high-frequency and discovered that SMG1 mutations tended to be concurrent with PIK3CA mutations in the ICD-high subtype, whereas PCDH15 mutations were often concurrent with CHRNB2 mutations (**Figure 3E**). In contrast, in the ICD-low subtype, TP53 mutations were generally mutually exclusive with mutations in KIF26B. For the ICD-low tumors, ARID1B mutations were inclined to concur with TTN mutations, while SPTA1 gene mutations

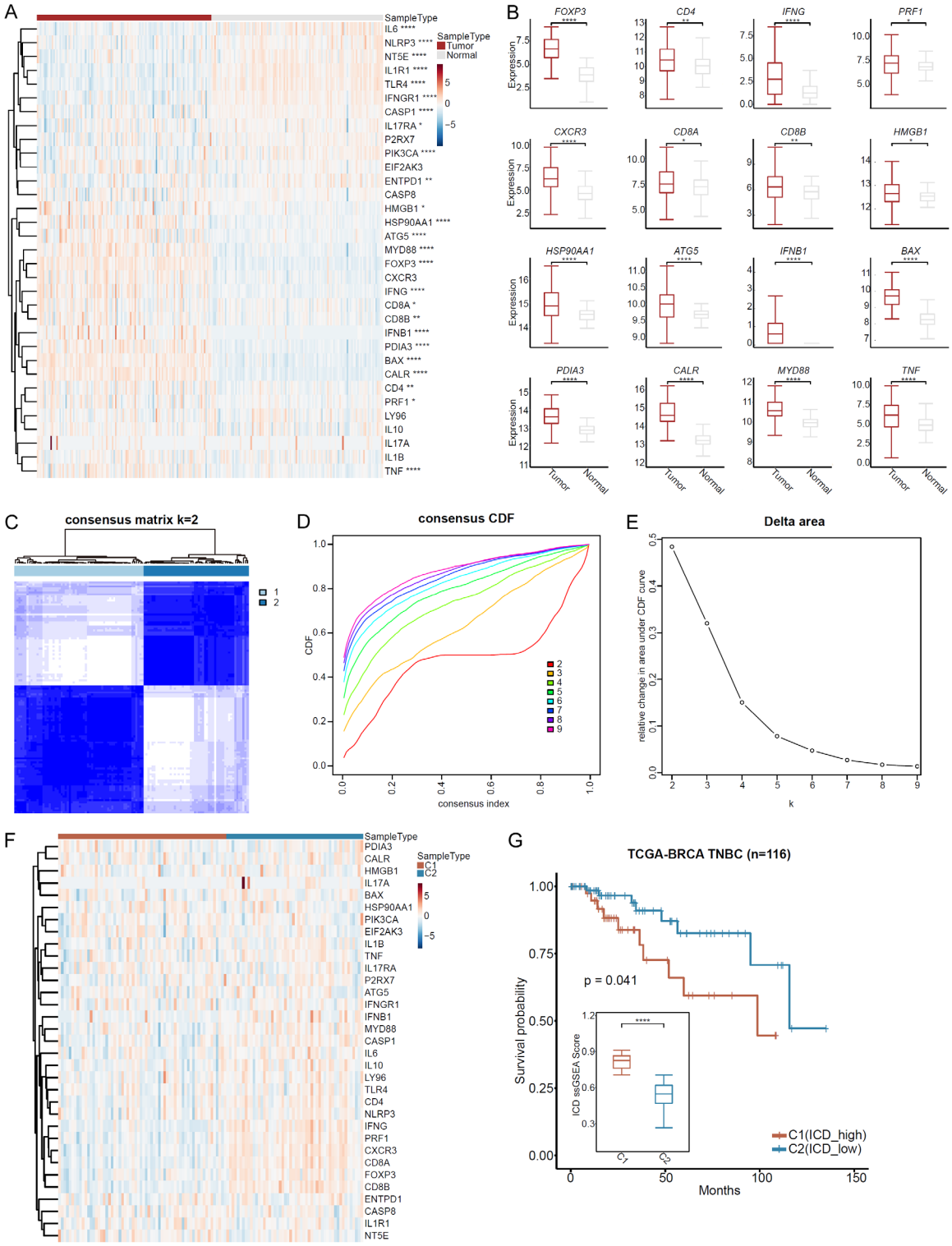

Figure 1. ICD-associated subtypes by consensus clustering. A. Heatmap plot shows the expression of 33 ICD-associated genes between TNBC and normal samples; B. Boxplots show 12 tumor-specific ICD-associated gene expression profiles among normal and TNBC samples in TCGA database; C. Heatmap depicts consensus clustering solution (k = 2) for 33 genes in TCGA TNBC samples; D, E. Delta area curve of consensus clustering indicates the relative change in area under the CDF curve for k = 2 to 9; F. Heatmap of 33 ICD-related gene expressions in different subtypes. Red represents high expression and blue represents low expression; G. Kaplan-Meier curves of OS in ICD-High and ICD-Low subtypes in the TCGA TNBC cohort. Abbreviations: ICD, Immunogenic cell death; TNBC, Triple-negative breast cancer; TCGA, The cancer genome atlas; CDF, Cumulative distribution function; OS, Overall survival; BRCA, Breast cancer. *P < 0.05, **P < 0.01, ***P < 0.001, & ****P < 0.0001.

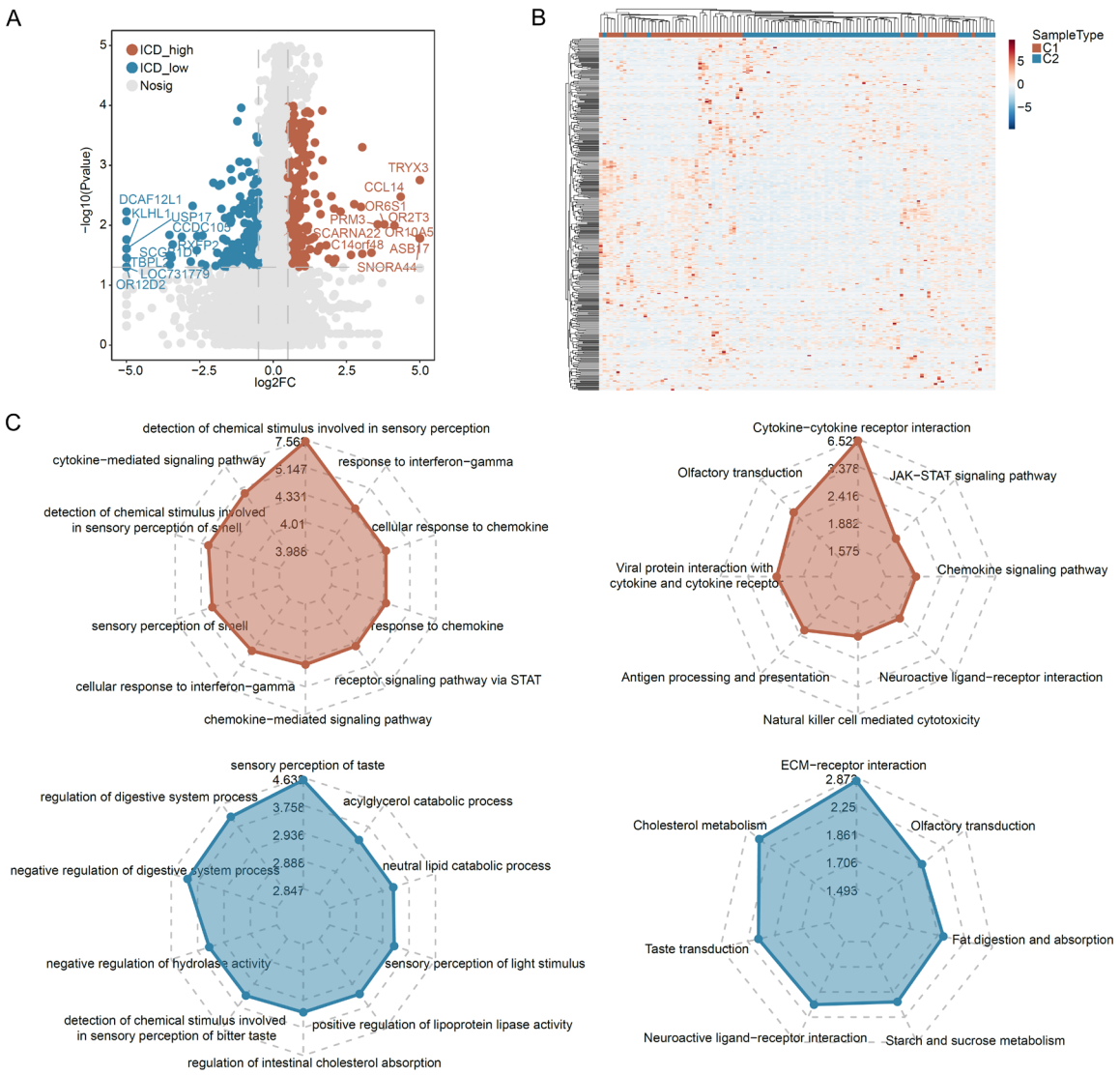

Figure 2. Identification of DEGs and underlying signal pathways in different subtypes. A. Volcano plot presents the distribution of DEGs quantified between ICD-high and ICD-low subtypes with a threshold of |log2 Fold change| > 0.25 and P < 0.05 in TCGA cohort; B. Heatmap shows the DEG expression in different subtypes; C. Radar plots present the GO (left) and KEGG (right) signaling pathway enrichment analysis. The layer represents -log10 (*p*. adjust-value), the orange color represents the ICD-High group, and the blue color represents the ICD-Low group. Abbreviations: DEGs, Differentially expressed genes; ICD, Immunogenic cell death; TCGA, The cancer genome atlas; GO, Gene ontology; KEGG, Kyoto encyclopedia of genes and genomes.

were inclined to concur with DLC1 or DNAH17 mutations (**Figure 3F**).

Microenvironment landscape in ICD-high and ICD-low subtypes

Since increasing evidence has demonstrated the effect of ICD in initiating the adaptive immune responses to eliminate tumor cells, we compared the composition of the TME between the two ICD subtypes. We found a higher immune score and a higher tumor heterogeneity in the ICD-high subtype than in the ICD-low subtype (**Figure 4A**). Then, we utilized TIMER combined with the LM22 signature matrix to assess the difference in the tumor infiltrating immune cells between these two ICD subtypes. **Figure 4B** shows the results of TNBC patients and normal samples from the TCGA cohort. As shown in **Figure 4C**, ICD-high subtype patients exhibited an increased proportion of memory B cells, M1 macrophage, activated memory CD4+

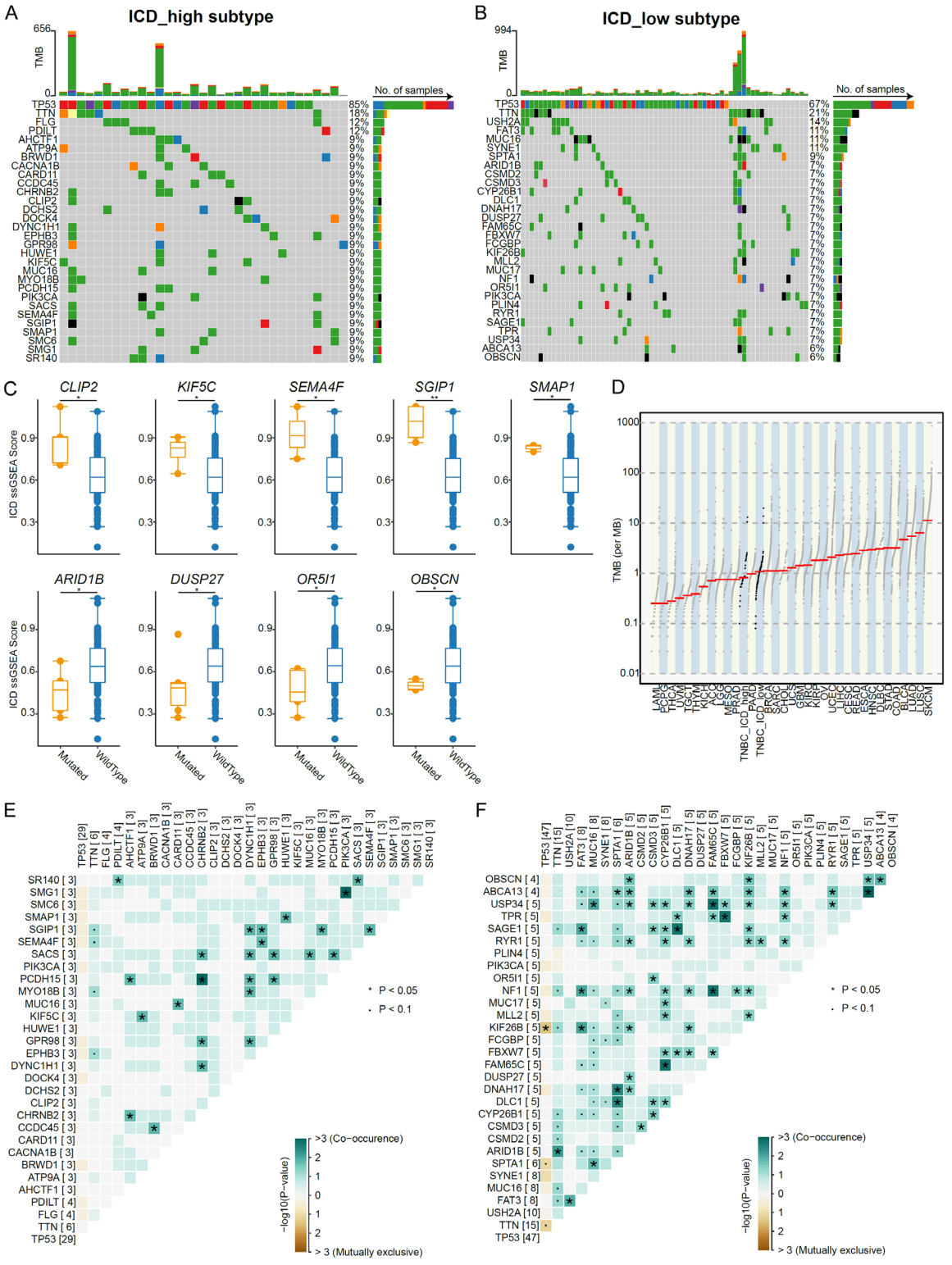

Figure 3. Genomic landscape related to ICD subtypes. (A, B) Comparison of the differences in the mutation status in the top 30 genes with mutations between ICD-High (A) and ICD-Low groups (B) in the TCGA TNBC cohort. Genes were ranked by mutation frequency. (C) Boxplots show that CLIP2, KIG5C, SEMA4F, SGIP1, and SMAP1 gene mutations were significantly correlated with high ICD signatures in the ICI-cohort, while ARID1B, DUSP27, OR5I1, and OBSCN gene mutations are significantly correlated with low ICD signature (Wilcoxon rank sum test). (D) Comparison of the TMB in TCGA pan-cancer cohort. (E, F) Concurrence (blue) and mutual exclusion (brown) between high-frequency mutation genes (the top 30 genes with mutations) in ICD-High (E) and ICD-Low (F) groups. Abbreviations: ICD, Immunogenic cell death; TCGA, The cancer genome atlas; TNBC, Triple-negative breast cancer; ICI, Immune checkpoint inhibitors; TMB, Tumor mutation burden. P < 0.1, *P < 0.05.

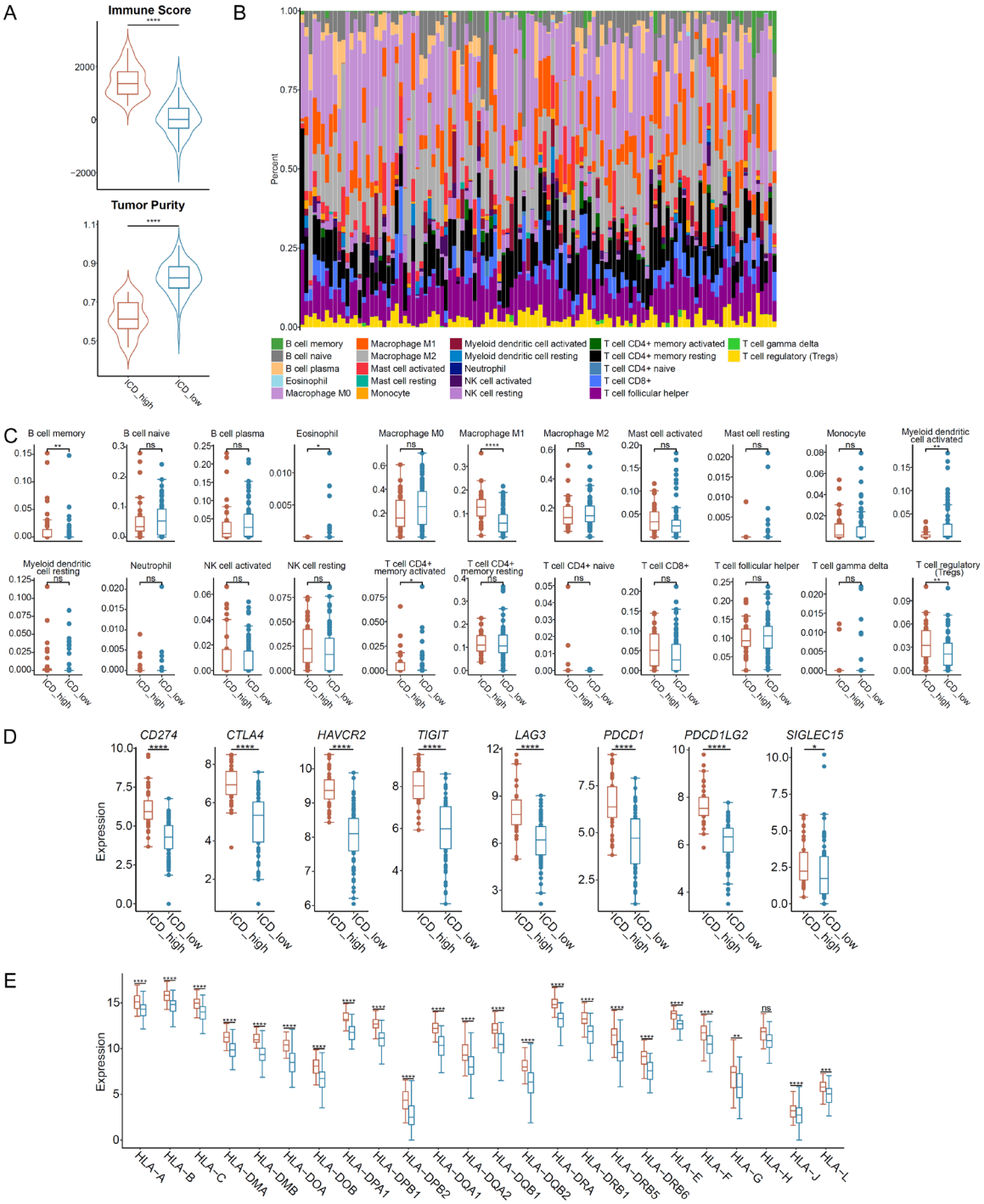

Figure 4. The immune landscape of ICD-High and ICD-Low subtypes. (A) Violin plots show the median, and quartile estimations for each immune score, and tumor purity score; (B) Relative proportion of immune infiltration in ICD-high and ICD-low subtypes; (C) Box plots visualize 22 immune cells between different subtypes; (D, E) Box plots present differential expression of multiple immune checkpoints (D), and HLA genes (E) between ICD-high and ICD-low subtypes. Abbreviations: ICD, Immunogenic cell death; HLA, Human leukocyte antigen. *P < 0.05, **P < 0.01, ***P < 0.001, and ****P < 0.0001.

T cells, and Tregs. Additionally, most of the immune checkpoints and the human leukocyte antigen (HLA) genes were highly expressed in the ICD-high subtype. In contrast, the ICD-low

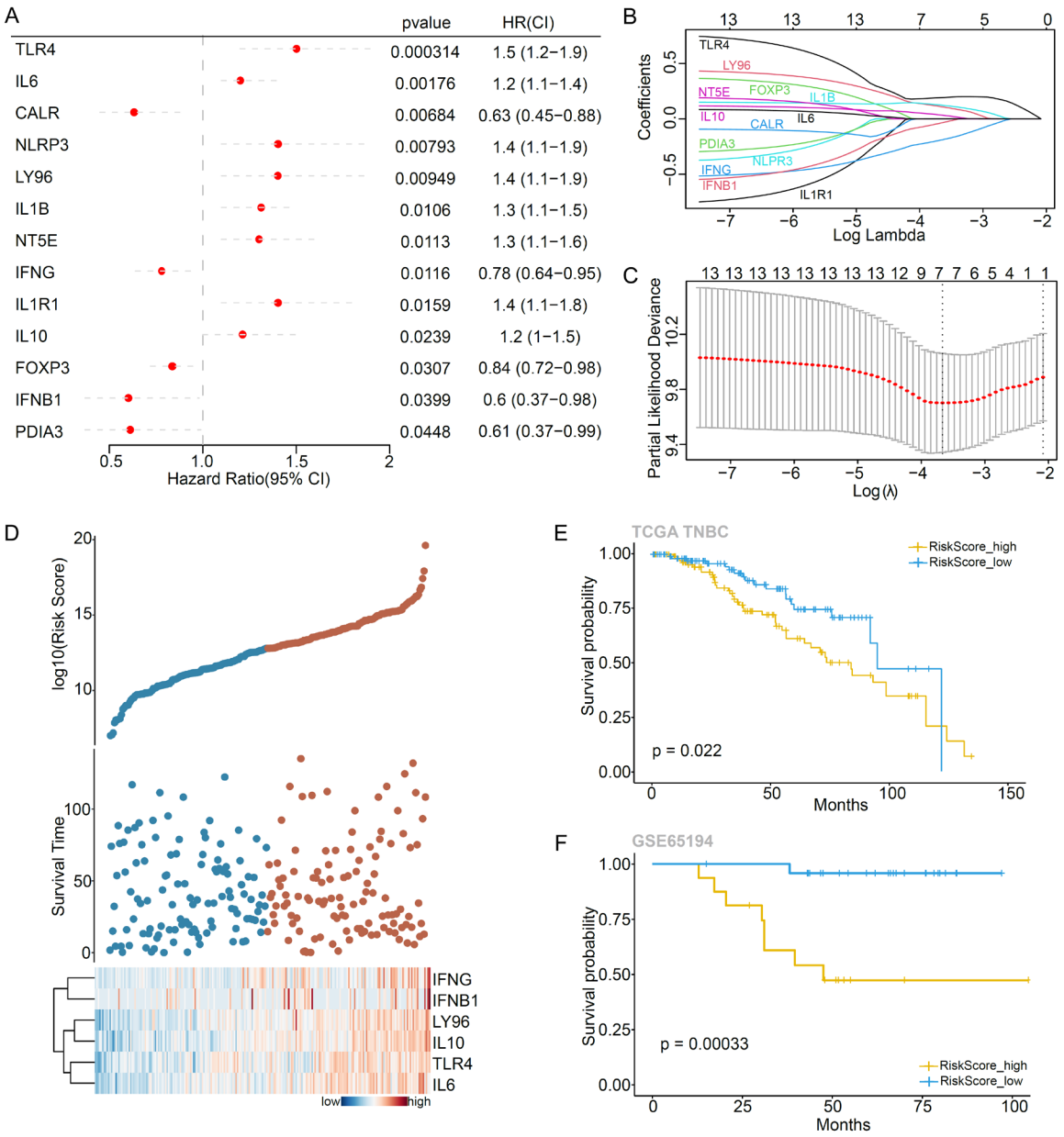

Figure 5. Construction and validation of the ICD risk signature. A. Univariate Cox analysis evaluates the prognostic value of the ICD genes in terms of OS; B, C. Lasso Cox analysis identified 13 genes most associated with OS in TCGA dataset; D. Risk score distribution, survival status of each patient, and heatmaps of prognostic 5-gene signature in TCGA database; E, F. Kaplan-Meier analyses demonstrate the prognostic significance of the risk model in TCGA and GSE65194 cohort. Abbreviations: HR, Hazard ratio; ICD, Immunogenic cell death; OS, Overall survival; Lasso, Least absolute shrinkage and selection operator; TCGA, The cancer genome atlas.

subtype exhibited the opposite results (**Figure 4D**, **4E**). Together, these results demonstrated that the ICD-high subtype was related to the intense immune phenotype, while the ICD-low subtype was related to the weakened immune phenotype.

Generation and validation of the ICD risk signature

We further established a prognostic model based on the genes associated with ICD. First, the univariate Cox analysis revealed that 13

ICD-associated genes were strongly related to the survival of patients (**Figure 5A**). We then tested the ICD-related genes and utilized them in LASSO regression analysis to construct the prediction model (**Figure 5B**, **5C**). The risk scores were calculated based on the algorithm: Risk score = 0.30048840 * LY96 + (-0.29873897) * IFNG + 0.09035484 * TLR4 + (-0.24929602) * IFNB1 + 0.06176552 * IL6. Importantly, we further analyzed the association of the risk score with survival status and found that the low-risk score cohort had more samples with alive status than that in the high-risk score cohort (**Figure 5D**). The prognostic value of the ICD risk signature in TNBC was further evaluated by using KM analysis (**Figure 5E**). According to analysis with TCGA samples, the high-risk score group exhibited a poor OS, consistent with the data in the GEO dataset (**Figure 5F**).

The immune landscapes of the ICD-high and ICD-low subtypes

Given the role that ICD plays in antitumor immunity, we exploited the correlation between ICD risk score and TME. Our results demonstrated that patients with high-risk score presented a positive correlation with M1 macrophages, activated memory CD4+ T cells, and CD8+ T cells (**Figure 6A**). Furthermore, we verified these results in the GEO cohort (**Figure 6B**). Moreover, we determined the predictive value of the ICD risk signature in immunotherapy efficacy by using TIDE and revealed that the ICD high-risk group had the highest response rate to immunotherapy in the immunotherapy response group, indicating that groups at high risk could be more likely to benefit from immunotherapy compared to groups at low risk (**Figure 6C**).

Discussion

The characteristic of immunogenic cell death (ICD) is the secretion of DAMPs to the immune system, where DAMPs attract and activate innate immune cells via interaction with various PRRs, as well as subsequently present antigens to T cells to trigger the immune response [5, 6]. As a result, ICD plays an important role in eliciting the host immune system to exert an anticancer response [19]. Accordingly, many studies have focused on the immunotherapeutic application of ICD, and many novel immunotherapeutic regimens for ICD have been proposed [18, 20, 21]. Therefore, it is critical to identify ICD-related biomarkers that will predict the efficacy of ICD immunotherapy in patients with TNBC. In this study, we confirmed that the expression of ICD-associated genes was intimately correlated with the clinical outcomes and the TME of TNBC. Our study also classified the tumors into ICD-high and ICD-low subtypes by consensus clustering of the ICD-associated genes. We showed that ICD-high subtype was enriched in tumor infiltrating immune cells and had upregulated expression of immune checkpoints, which might show a better response to immunotherapy. In addition, we constructed a prognostic risk signature with 33 ICD-associated genes, which was used to divide the TNBC patients into two ICD subgroups. Furthermore, this risk signature was verified in predicting the prognosis of patients with TNBC. Our results supported the findings from other studies. For example, it was reported that a signature consisting of 34 ICD-associated genes was correlated with the survival of women with ovarian cancer, breast cancer, and lung cancer. Additionally, a significant association was found between some of the ICD-associated genes, e.g., LY96, IFNG, TLR4, IFNB1, and IL6, and the immune-active microenvironment in TNBC patients. Since tumor immunotherapy can induce anti-tumor immune responses and activate long-term immunological memory responses [22], immunotherapy has significantly changed the paradigm of cancer therapy. Nevertheless, a low response rate caused by an immunosuppressive tumor microenvironment is still a major barrier to overcome. Considering that ICD can attract innate immune cells and release DAMPs to promote DC maturation, T cell activation, and CTLs infiltration, which elicits antitumor immune responses [23, 24], we classified the patients into two ICD subtypes by consensus clustering. Of these, the ICD-high subtype showed an immune-active microenvironment, while the ICD-low subtype presented an immune-suppressive microenvironment.

In summary, our results reveal the correlation of ICD subgroups with the alterations in the immune microenvironment of patients with TNBC. This finding might guide clinicians in the selection of immunotherapy for the treatment of TNBC patients. Furthermore, our study pro-

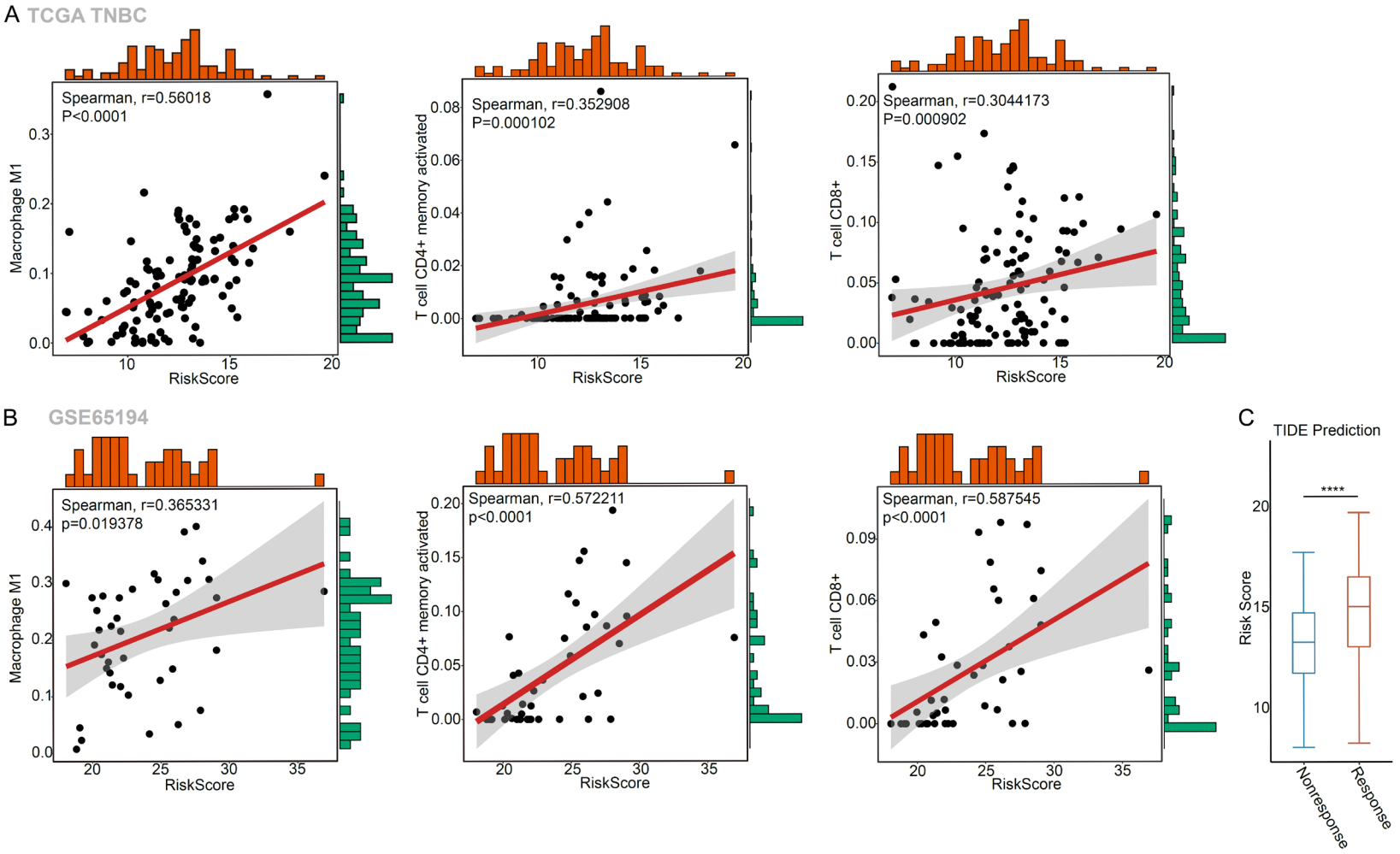

Figure 6. Association of ICD risk signature with the tumor microenvironment. (A, B) Scatter plots show the correlation of risk score with the infiltration of macrophages M1, T cells CD4+ memory activated, and T cells CD8+ in the TCGA TNBC cohort (A), and further validated in the GSE65194 cohort (B); (C) Box plot presents the association of ICD risk score with immunotherapy response. Abbreviations: ICD, Immunogenic cell death; TCGA, The cancer genome atlas; TNBC, Triple-negative breast cancer; TIDE, Tumor immune dysfunction and exclusion.

poses a classification system based on the ICD-related signature to predict the prognosis and immunotherapeutic response which may be useful in clinical practice.

Acknowledgements

The results published here are in part based on data generated by the TCGA Research Network (https://www.cancer.gov/tcga). Supported by the National Natural Science Foundation of China (Grant Nos. 82072931 and 82002805).

Disclosure of conflict of interest

None.

Address correspondence to: Xiao-An Liu, Department of Breast Surgery, The First Affiliated Hospital of Nanjing Medical University, 300 Guangzhou Road, Nanjing 210029, Jiangsu, China. E-mail: liuxiaoan@126.com

References

[1] Galluzzi L, Buque A, Kepp O, Zitvogel L and Kroemer G. Immunogenic cell death in cancer and infectious disease. Nat Rev Immunol 2017; 17: 97-111.

[2] Green DR, Ferguson T, Zitvogel L and Kroemer G. Immunogenic and tolerogenic cell death. Nat Rev Immunol 2009; 9: 353-363.

[3] Yatim N, Cullen S and Albert ML. Dying cells actively regulate adaptive immune responses. Nat Rev Immunol 2017; 17: 262-275.

[4] Galluzzi L, Vitale I, Warren S, Adjemian S, Agostinis P, Martinez AB, Chan TA, Coukos G, Demaria S, Deutsch E, Draganov D, Edelson RL, Formenti SC, Fucikova J, Gabriele L, Gaipl US, Gameiro SR, Garg AD, Golden E, Han J, Harrington KJ, Hemminki A, Hodge JW, Hossain DMS, Illidge T, Karin M, Kaufman HL, Kepp O, Kroemer G, Lasarte JJ, Loi S, Lotze MT, Manic G, Merghoub T, Melcher AA, Mossman KL, Prosper F, Rekdal O, Rescigno M, Riganti C, Sistigu A, Smyth MJ, Spisek R, Stagg J, Strauss BE, Tang D, Tatsuno K, van Gool SW, Vandenabeele P, Yamazaki T, Zamarin D, Zitvogel L, Cesano A and Marincola FM. Consensus guidelines for the definition, detection and interpretation of immunogenic cell death. J Immunother Cancer 2020; 8: e000337.

[5] Gong T, Liu L, Jiang W and Zhou R. DAMP-sensing receptors in sterile inflammation and inflammatory diseases. Nat Rev Immunol 2020; 20: 95-112.

[6] Paludan SR, Reinert LS and Hornung V. DNA-stimulated cell death: implications for host defence, inflammatory diseases and cancer. Nat Rev Immunol 2019; 19: 141-153.

[7] West AP and Shadel GS. Mitochondrial DNA in innate immune responses and inflammatory pathology. Nat Rev Immunol 2017; 17: 363-375.

[8] Galluzzi L, Buque A, Kepp O, Zitvogel L and Kroemer G. Immunological effects of conventional chemotherapy and targeted anticancer agents. Cancer Cell 2015; 28: 690-714.

[9] Ye W, Gunti S, Allen CT, Hong Y, Clavijo PE, Van Waes C and Schmitt NC. ASTX660, an antagonist of cIAP1/2 and XIAP, increases antigen processing machinery and can enhance radiation-induced immunogenic cell death in preclinical models of head and neck cancer. Oncoimmunology 2020; 9: 1710398.

[10] Xiao R, Allen CT, Tran L, Patel P, Park SJ, Chen Z, Van Waes C and Schmitt NC. Antagonist of cIAP1/2 and XIAP enhances anti-tumor immunity when combined with radiation and PD-1 blockade in a syngeneic model of head and neck cancer. Oncoimmunology 2018; 7: e1471440.

[11] Galluzzi L, Humeau J, Buque A, Zitvogel L and Kroemer G. Immunostimulation with chemotherapy in the era of immune checkpoint inhibitors. Nat Rev Clin Oncol 2020; 17: 725-741.

[12] Pol J, Vacchelli E, Aranda F, Castoldi F, Eggermont A, Cremer I, Sautes-Fridman C, Fucikova J, Galon J, Spisek R, Tartour E, Zitvogel L, Kroemer G and Galluzzi L. Trial watch: immunogenic cell death inducers for anticancer chemotherapy. Oncoimmunology 2015; 4: e1008866.

[13] Gluz O, Liedtke C, Gottschalk N, Pusztai L, Nitz U and Harbeck N. Triple-negative breast cancer--current status and future directions. Ann Oncol 2009; 20: 1913-1927.

[14] So JY, Ohm J, Lipkowitz S and Yang L. Triple negative breast cancer (TNBC): non-genetic tumor heterogeneity and immune microenvironment: emerging treatment options. Pharmacol Ther 2022; 237: 108253.

[15] Mezni E, Behi K and Goncalves A. Immunotherapy and breast cancer: an overview. Curr Opin Oncol 2022; 34: 587-594.

[16] Zhang X, Ge X, Jiang T, Yang R and Li S. Research progress on immunotherapy in triple-negative breast cancer (Review). Int J Oncol 2022; 61: 95.

[17] Lu JY, Alvarez Soto A and Anampa JD. The landscape of systemic therapy for early stage triple-negative breast cancer. Expert Opin Pharmacother 2022; 23: 1291-1303.

[18] Pathak N, Sharma A, Elavarasi A, Sankar J, Deo SVS, Sharma DN, Mathur S, Kumar S, Prasad CP, Kumar A and Batra A. Moment of

truth-adding carboplatin to neoadjuvant/adjuvant chemotherapy in triple negative breast cancer improves overall survival: an individual participant data and trial-level meta-analysis. Breast 2022; 64: 7-18.
[19] Fucikova J, Moserova I, Urbanova L, Bezu L, Kepp O, Cremer I, Salek C, Strnad P, Kroemer G, Galluzzi L and Spisek R. Prognostic and predictive value of DAMPs and DAMP-associated processes in cancer. Front Immunol 2015; 6: 402.
[20] Li Y, Zhang H, Li Q, Zou P, Huang X, Wu C and Tan L. CDK12/13 inhibition induces immunogenic cell death and enhances anti-PD-1 anticancer activity in breast cancer. Cancer Lett 2020; 495: 12-21.
[21] Kroemer G, Galluzzi L, Kepp O and Zitvogel L. Immunogenic cell death in cancer therapy. Annu Rev Immunol 2013; 31: 51-72.
[22] Li Z, Lai X, Fu S, Ren L, Cai H, Zhang H, Gu Z, Ma X and Luo K. Immunogenic cell death activates the tumor immune microenvironment to boost the immunotherapy efficiency. Adv Sci (Weinh) 2022; 9: e2201734.
[23] Serrano-Del Valle A, Anel A, Naval J and Marzo I. Immunogenic cell death and immunotherapy of multiple myeloma. Front Cell Dev Biol 2019; 7: 50.
[24] Rodrigues MC, Morais JAV, Ganassin R, Oliveira GRT, Costa FC, Morais AAC, Silveira AP, Silva VCM, Longo JPF and Muehlmann LA. An overview on immunogenic cell death in cancer biology and therapy. Pharmaceutics 2022; 14: 1564.